

Discovery of Novel Alanine Aminotransferase and Aspartate Aminotransferase Inhibitors by Large Scales Docking-Based Virtual Screening

Faezeh Sadat Hosseini¹, Houman Kazemzadeh¹, Parisa Shahsavari¹, Mina Gholami¹, Zinat Bahrampour Omrany¹, Arash Amanlou², Massoud Amanlou^{1,2,*} 

¹ Department of Medicinal Chemistry, Faculty of Pharmacy, Tehran University of Medical Sciences, Tehran, Iran

² Experimental Medicine Research Center, Tehran University of Medical Sciences, Tehran, Iran

* Correspondence: amanlou@tums.ac.ir (M.A.);

Scopus Author ID 6603321293

Received: 26.08.2022; Accepted: 7.10.2022; Published: 22.11.2022

Abstract: Alanine aminotransferase (ALT) and aspartate aminotransferase (AST) is the cardinal enzymes in the liver and play a substantial role in balancing many metabolic pathways. A peccadillo, in the activity of these enzymes, can end up in uncontrollable challenges like chronic conditions. Therefore, the demand to use small molecules to control the enzyme's activity and prevent the mentioned challenges will be undeniable in the future. To answer this demand, a large scales virtual screening procedure, using molecular docking of 9127 FDA and world-approved drugs, including herbal medicine, was performed using Autodock 4.2 over the crystal structures of ALT and AST (PDB ID: 7AAT, 3IHJ respectively). The results revealed that small molecule xanthurenic acid- β -glucoside with quinoline monocarboxylic acid backbone and glucoside substitution could fit well in both active sites of ALT and AST and interact properly with the most key residues. These features, accompanied by suitable ADME properties, lower toxicity than previously reported inhibitors, and neoteric general backbone, make them potential candidates that can be used either as medicine in clinical trials or as a structural basis for designing other novel inhibitors.

Keywords: aspartate aminotransferase; alanine aminotransferase; inhibitors; chronic conditions; virtual screening.

© 2022 by the authors. This article is an open-access article distributed under the terms and conditions of the Creative Commons Attribution (CC BY) license (<https://creativecommons.org/licenses/by/4.0/>).

1. Introduction

The liver is a large, complex, and strategic organ well recognized for its dominant role in metabolism, excreting xenobiotics, synthesizing plasma proteins, and toxic detoxifying products [1,2]. The liver enzymes detoxify waste products through processes like amino acid deamination [2,3]. Two gluconeogenesis enzymes, alanine aminotransferase (ALT) and aspartate aminotransferase (AST), are the main enzymes responsible for detoxifying. Pyridoxal phosphate-dependent enzymes ALT and AST play vital roles in gluconeogenesis and amino acid metabolism in the liver. They catalyze glucose and protein metabolisms; ALT converts alanine into pyruvate and then converts pyruvate into acetate or acetyl-CoA via pyruvate decarboxylase. By the end of the aspartate metabolism, oxaloacetate and glutamate are produced along with AST [4-6]. Notably, ALT and AST is high throughout the body, but it is

mainly located in the liver (Figure 1), heart, skeletal muscles, kidney, brain, and red blood cells [7,8].

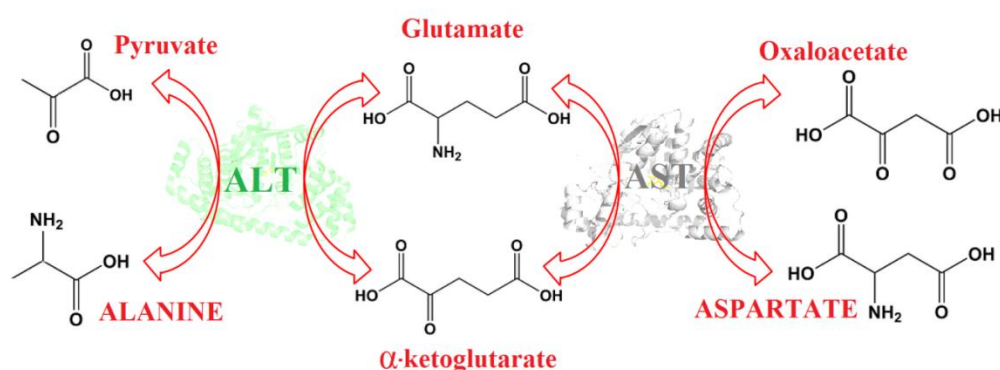


Figure 1. Metabolic function of alanine aminotransferase (ALT) and aspartate aminotransferase (AST).

Being an intracellular enzyme [9], playing a significant role in balancing metabolism, and abundant presence in many different cells, such as liver cells, enable us to use these enzymes as an indicator for measuring the health of many organs, mainly the liver [10], and as a target for designing new inhibitors [11]. Previous studies also approve that abnormal enzyme levels are involved in liver diseases, hypercholesterolemia [12], cancers [13], hypertension [14], skeletal muscle disorder [15], and other metabolic and non-metabolic diseases [4,16]. Diseases such as hypertension [17], skeletal muscle disorders [18], colon cancer [19], breast cancer [20], liver abnormalities [4], and pancreatic ductal adenocarcinoma (PDAC) [21] received more attention than other diseases as the studies indicate [22].

In this regard, scientists focused on designing a new paradigm to design, synthesize, and examine different chemicals by inhibiting these two gluconeogenesis enzymes and prevent or treat diseases related to the high level of ALT and AST afterward [16-26], but the major issues like toxicity didn't allow them to use them in clinical situations [26-28].

Therefore, the quest for finding novel inhibitors entered a new path. A path that could lead to finding inhibitors without the major issues observed in previous attempts and bearing novel backbones different from the previous ones [29,30].

Flavonoids were novel inhibitors that some studies insisted on considering as leading compounds for designing safe and effective drugs to manage increased ALT and AST-related disorders [2,31]. Our previous study on inhibiting liver alanine aminotransferase and aspartate aminotransferase effects of hesperidin and hesperetin, two major citrus flavonoids, also confirmed this idea [32].

In this study, we did a virtual screening using 9127 FDA and world-approved drugs, including some herbal medicine and some chemical compound with possible efficacy, over the crystal structures of ALT and AST to find novel potential small molecules that could have desirable inhibition on the two gluconeogenesis enzymes. The result indicates xanthurenic acid- β -glucoside with quinoline monocarboxylic acid backbone and glucoside substitution can fit well and interact properly with the most key residues in both active sites of ALT and AST enzymes.

2. Materials and Methods

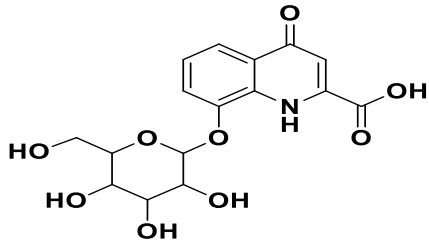
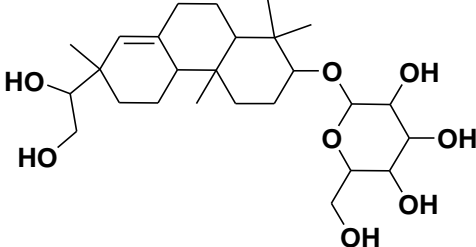
For the sake of discovering new potential inhibitors that will interact with the active site of the ALT and AST, the 3D structure of 9127 FDA-approved drugs, world-approved drugs, regulated chemicals, and herbal isolates was retrieved from the SWEETLEAD database

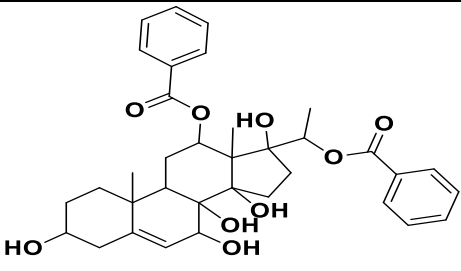
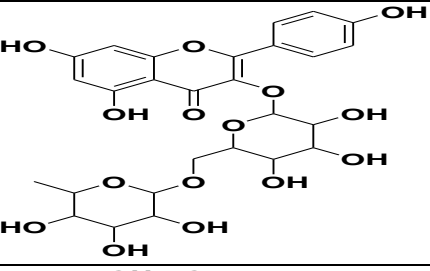
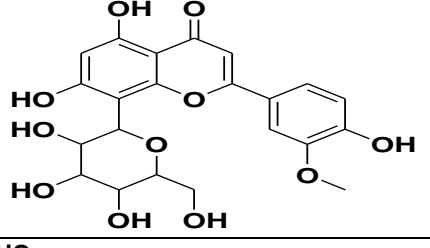
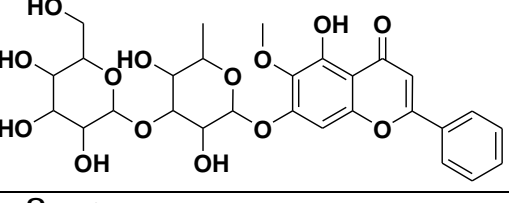
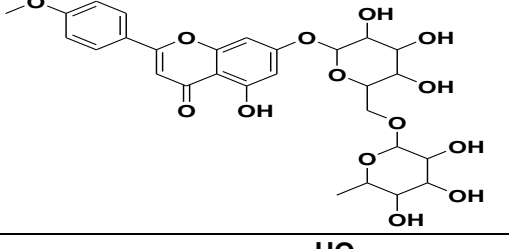
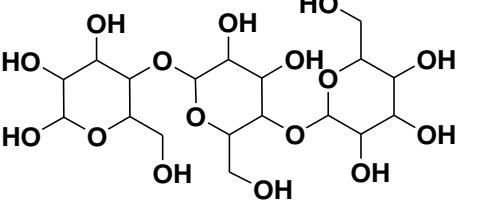
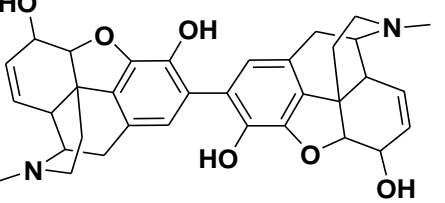
[33] and screened with molecular docking simulations after preparation. AutoDockTools (ADT, Ver.1.5.6) was used to prepare the input files and analyze the results[34]. The downloaded 3D structure of the ligands was in structure data file (SDF) format. So, OpenBabel (version 2.3.1) [35] converted SDF to PDB format. After that, rotatable bonds and Gasteiger charges were assigned, and the prepared file was saved in pdbqt format. To prepare the protein input files, the crystal structure of ALT and AST with PDB ID: 3IHJ, and 7AAT, respectively, were downloaded from The RCSB website (<https://www.rcsb.org>). Then all the water molecules were removed from the PDB files, polar hydrogen was added, and the Kollman-united charge [36-39] calculated the partial atomic charge. The prepared files were saved in pdbqt format to be used in the following steps. AutoDock 4.2 and AutoGrid 4.2 were used to perform docking simulations and generate grid maps. All the docking parameters were set as their default value except for the running jobs set for 10 runs. Grid box $50 \times 50 \times 50 \text{ \AA}$ (x, y, and z) with 0.375 nm spacing for each dimension was positioned on the active site of the ALT and AST. Based on their score, the ten best docking binding energy results were arranged from the lowest to highest. Docking procedures were done automatically by scripts written in-house. The docking results are visualized by Discovery Studio visualizer version 17.2 [40] and PyMol version 1.1level [41].

3. Results and Discussion

Virtual screening was performed over the 9127 ligands from the SWEETLEAD database on both ALT and AST active sites. The docking results were ranked the compounds according to the lowest to highest docking binding energy, and each enzyme was investigated separately. The top 10 compounds from ALT and AST enzymes are listed in Table 1 and Table 2, respectively.

Table 1. Top ten potential inhibitors from virtual screening of SWEETLEAD databases over alanine aminotransferase (ALT, 3IHJ).

No.	Structure	Compound name	Binding energy (kcal/mol)	Residue of action
1		Xanthurenic acid- β -glucoside	-10.65	H bonds: Leu 218, Tyr 216, Tyr 440 Pi interactions: Pro 217 Attractive charge: Arg 494 Van der Waals: Phe 484, Asn 94, Asn 271
2		Darutoside	-10.29	H bonds: PLP, Tyr 216, Ser 340, Arg 350 Pi interactions: Pro 217 Van der Waals: leu 218, Ser 188

No.	Structure	Compound name	Binding energy (kcal/mol)	Residue of action
3		Dibenzoylelgaimol	-10.16	H bonds: Ser 188 Pi interactions: Tyr 216, Arg 494 Van der Waals: Tyr 440, Met 439, Asn 94
4		Kaempferol-3-robinobioside	-9.89	H bonds: Ser 188, Asn 94, Tyr 440 Pi interactions: Pro 217, Arg 350 Van der Waals: Lys 341, Ser 340, Tyr 302
5		Scoparin	-9.71	H bonds: Tyr 216, Tyr 302, leu 218 Pi interactions: PLP Van der Waals: Tyr 440, Phe 484, Arg 350
6		7-methoxybaicalein	-9.68	H bonds: Asn 271, Arg 494 Pi interactions: PLP, Pro 217 Van der Waals: Arg 350, Phe 484, Tyr 216
7		Linarin	-9.51	H bonds: Arg 350, Ser 188, Tyr 216, Tyr 440 Pi interactions: Leu 218, Pro 217 Van der Waals: Cys 347, Lys 341, Phe 484
8		Glucan	-9.48	H bonds: PLP, Asn 271, Ser 340 Van der Waals: Met 439, Asn 94, Arg 350
9		Pseudomorphone	-9.42	H bonds: PLP, Tyr 302, Tyr 440 Pi interactions: Leu 498 Van der Waals: Asn 271, Thr 496, Pro 217

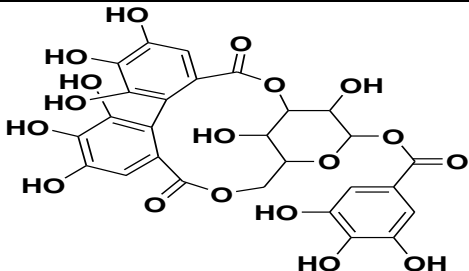
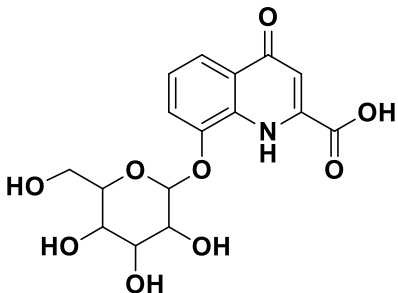
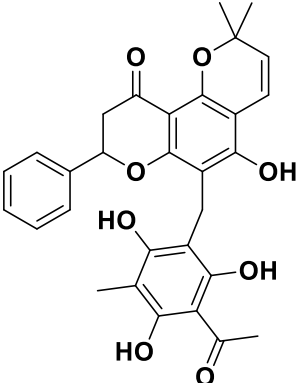
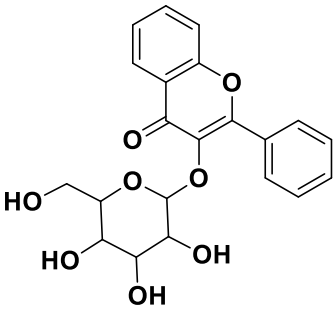
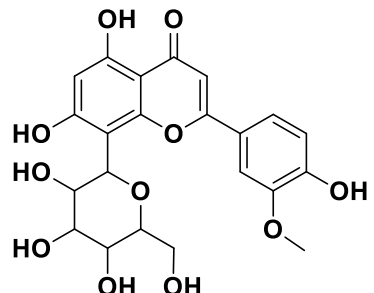
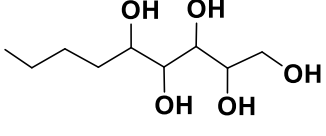
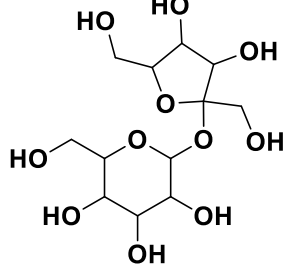
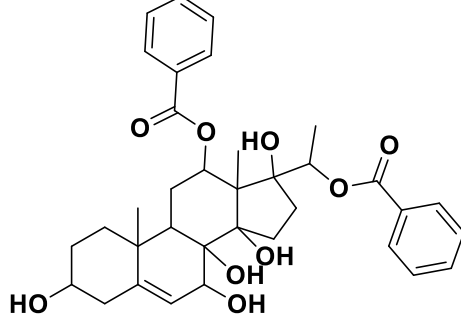
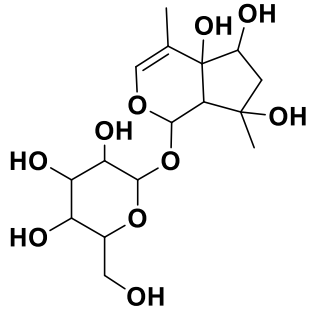
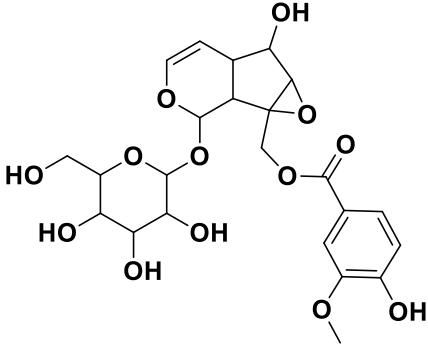
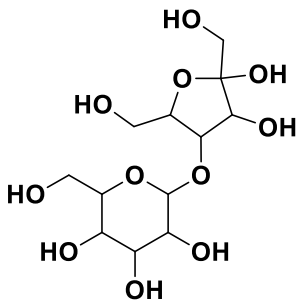
No.	Structure	Compound name	Binding energy (kcal/mol)	Residue of action
10		Corilagin	-9.40	H bonds: PLP, Asn 94, Tyr 440 Pi interactions: Tyr 216, Leu 218 Van der Waals: Lys 347, Tyr 341, Pro 217

Table 2. Top ten potential inhibitors from virtual screening of SWEETLEAD databases over aspartate aminotransferase (AST, 7AAT).

No.	Structure	Compound name	Binding energy (kcal/mol)	Residue of action
1		Xanthurenic acid-β-glucoside	-10.11	H bonds: Trp 140 Pi interactions: Ile 17 Salt bridge: Arg 386 Van der Waals: Phe 360, Ala 39, Tyr 263
2		Isorottlerin	-9.91	H bonds: Trp 140, Arg 266, Gly 38 Pi interactions: Ile 17, Phe 360, Tyr 263 Van der Waals: Asn 142, Met 359, Gly 264
3		Flavonol 3-o-glycosides	-9.55	H bonds: PLP, Tyr 225 Pi interactions: Trp 140 Van der Waals: Arg 386, Phe 360, Arg 266

No.	Structure	Compound name	Binding energy (kcal/mol)	Residue of action
4		Scoparin	-9.29	H bonds: Arg 266, Asn 142, Thr 109, Arg 386 Pi interactions: PLP, Gly 38 Van der Waals: Phe 360, Ile 17, Trp 140
5		Glucononitol	-9.27	H bonds: PLP, Trp 140 Van der Waals: Phe 360, Tyr 263, Ala 257
6		Sucrose	-9.25	H bonds: PLP, Gly 38, Asn 194 Van der Waals: Phe 360, Arg 266, Trp 140
7		Dibenzoylgagaimol	-9.10	H bonds: Gly 38, Tyr 225 Pi interactions: Trp 140, Ile 17, Ala 39 Van der Waals: Phe 360, Arg 386, Gly 141
8		Lamiol	-9.09	H bonds: PLP, Gly 38, Arg 386 Pi interactions: Ile 17 Van der Waals: Phe 360, Tyr 263, Trp 140

No.	Structure	Compound name	Binding energy (kcal/mol)	Residue of action
9		Kutkoside	-9.07	H bonds: PLP, Asn 194, Arg 386 Pi interactions: Ile 17, Trp 140 Van der Waals: Phe 360, Gly 38, Tyr 225
10		Lactulose	-9.07	H bonds: Gly 38, Asn 194, Arg 386 Van der Waals: Phe 360, Tyr 225, Ile 17

Two grooves access the active sites of ALT. Each monomer contains an equivalent active center with pyridoxal-5'-phosphate (PLP) with the intact Schiff base linkage between Lys 240 and PLP, and the electrostatic interactions that secure the binding of PLP to its phosphate moiety (including Ser 105, Ser 239, Arg 248 and Tyr 68, and the backbone amides of Val 104 and Ser 105), the covalent bond with Lys 240 induce a strained conformation in PLP, which in turn enhances its reactivity, further supported by an extended network of polar and non-polar interactions. Important residues that contribute to the active site include Ala 187, Ser 188, Asn 271, Asp 299, Tyr 302, Ser 338, and Arg 494. During the creation of interactions, the active site changes and catalyzes [8,42]. AST is a homodimer with two independent, active sites that mirror each other at the opposite sides of the enzyme[43]. The active sites are clefts that are fabricated from bordering the large domains of both subunits (involving residues 76-300) and the small domain of one subunit (involving residues 15-47 and 359-410) [44]. Important residues that contribute to the active site include Gly 38, Ser 107, Gly 108, Thr 109, Trp 140, His 143, Asp 194, Asp 222, Tyr 225, Ser 255, Lys 258, Phe 360, and Arg 386 [45, 46]. The main interaction of PLP with the active sites is through covalent bonds with Lys 258 [47]. These residues in the pocket of the active site help the substrate to bring into the pocket by interacting with the guanidinium moieties of Arg 292 [46]. The active site twitches (Figure 2) and catalysis occur when the interactions are created [45]. Now, it can be understood how top ligands have the lowest binding energy among all other compounds in the titled database over the ALT and AST active sites.

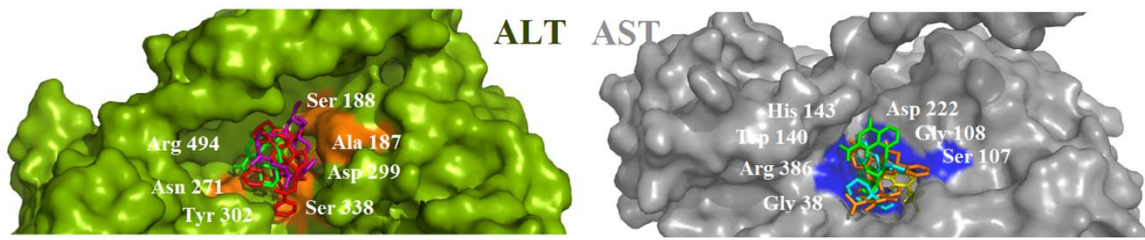


Figure 2. Displayed the active site of alanine aminotransferase (ALT) and aspartate aminotransferase (AST).

For the retrieved top ten compounds from virtual screening over the ALT, the docking binding energy has shown a range from -10.65 to -9.40 kcal/mol, and the range for AST was from -10.11 to -9.07 kcal/mol.

From the previous study, we know that hesperidin can properly fit in the active site of ALT with a binding energy of -5.7 kcal/mol, while hesperetin shows more ability to interact with the active site of the AST with a binding energy of -5.86 kcal/mol [32]. This is because hesperidin and hesperetin both have a flavonoid backbone in their structure.

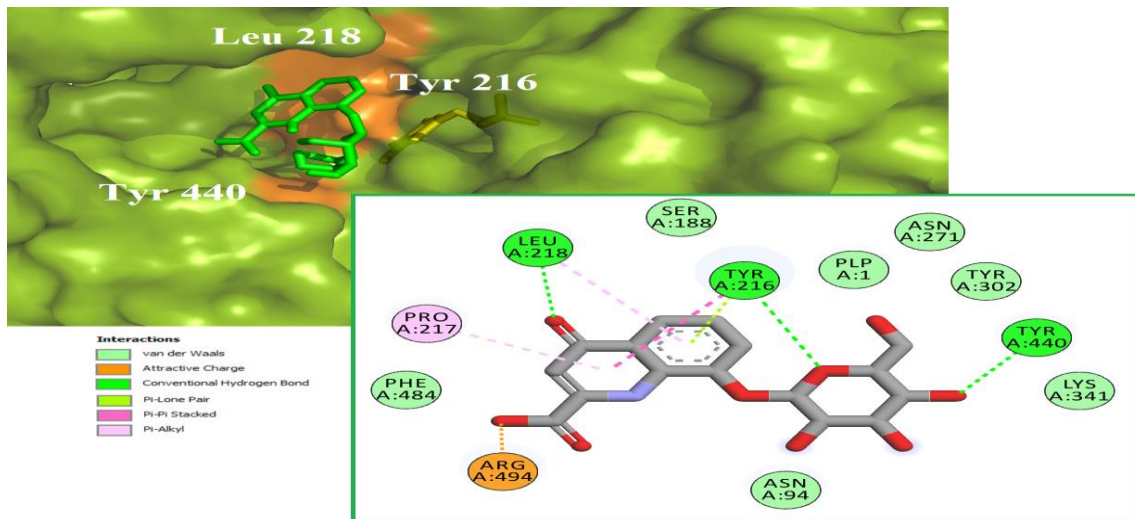


Figure 3. 2D and 3D views of the interaction between xanthurenic acid-β-glucoside and the active site of alanine aminotransferase (ALT), and pyridoxal-5'-phosphate (PLP) are shown with a yellow stick.

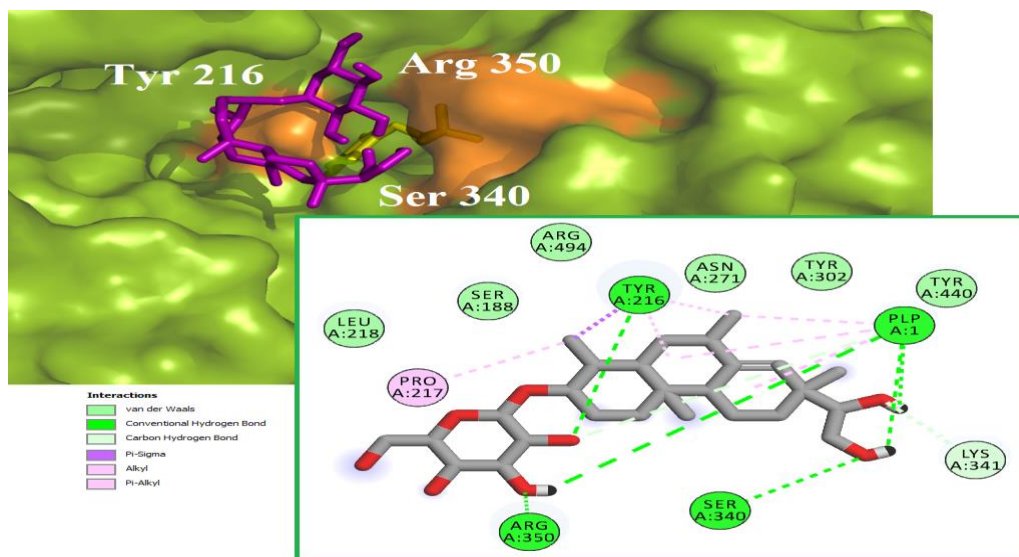


Figure 4. 2D and 3D view of the interaction between darutoside and the active site of alanine aminotransferase (ALT), and pyridoxal-5'-phosphate (PLP) shown in yellow stick.

Xanthurenic acid- β -glucoside with quinoline monocarboxylic acid backbone was previously known as the natriuretic agent [48] and the vasoactive compound [49], which indicates the significant affinity in the active site of ALT with the lowest binding energy. The docking conformation showed (Figure 3) the three hydrogen bonds with Tyr 216, leu 218, and Tyr 440 and the charge bond with Arg 494. Pi interactions were also formed with Tyr 216 and Pro 217. Several Van der Waals bonds were observed, especially with PLP.

A second potential ALT inhibitor based on the binding energy was darutoside with phenanthrene scaffold. Darutoside is the active ingredient of the Chinese traditional medicine of *Siegesbeckia pubescens* Makino along with hesperidin and contributes to the anti-inflammatory and antinociceptive activities [50]. Darutoside formed four hydrogen bonds with Tyr 216, Ser 340, Arg 350, and PLP moiety (Figure 4). The same Pi interactions, like xanthurenic acid- β -glucoside, were also observed with Tyr 216 and Pro 217, and several Van der Waals bonds were formed.

Interestingly the top retrieved potential inhibitor with the lowest binding energy in the active site of AST was the same as the ALT top potential inhibitor. Xanthurenic acid- β -glucoside forms a hydrogen bond with Trp140 and several Van der Waals bonds with Gly 38, Gly141, Asn 142, Asn 194, Tyr 225, Lys 258, Tyr 263, and PLP. Pi interaction was also observed with Ile 17 (Figure 5).

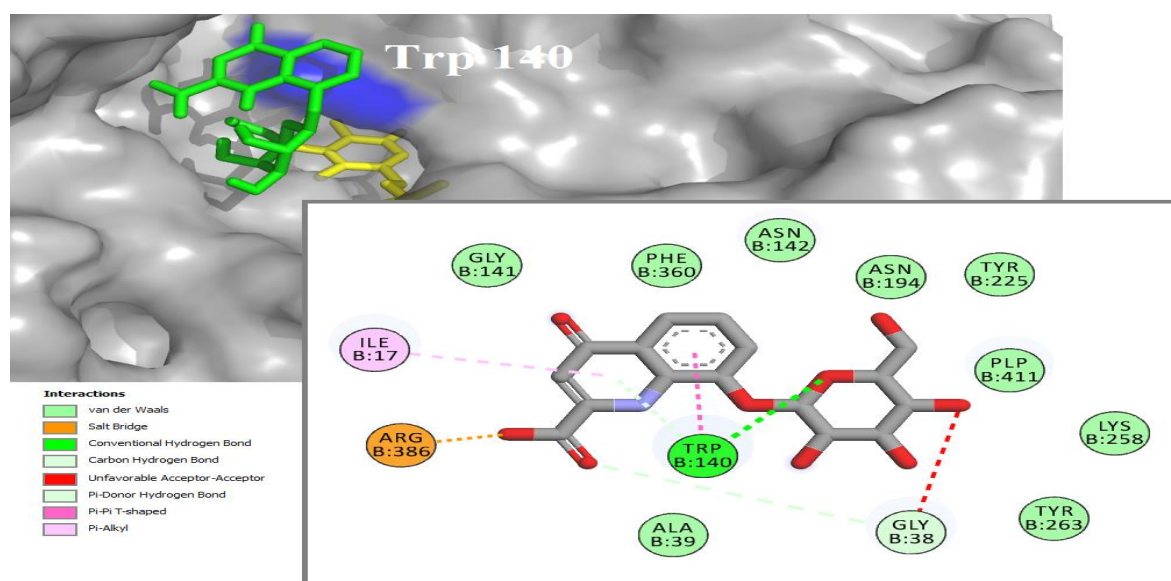


Figure 5. 2D and 3D views of the interaction between xanthurenic acid- β -glucoside and the active site of aspartate aminotransferase (AST) and pyridoxal-5'-phosphate (PLP) are shown in the yellow stick.

Isorottlerin was isolated from *Mallotus philippinensis* and identified as the anti-*H. pylori* [51] and anti-tuberculosis agents [52]. Three hydrogen bonds with Gly 38, Trp 140, Arg 266 were formed with the active site of the AST and isorottlerin. Moreover, a pi interaction was observed with Ile17, Tyr 263, and Phe 360, and also multiple Van der Waals interactions were generated (Figure 6).

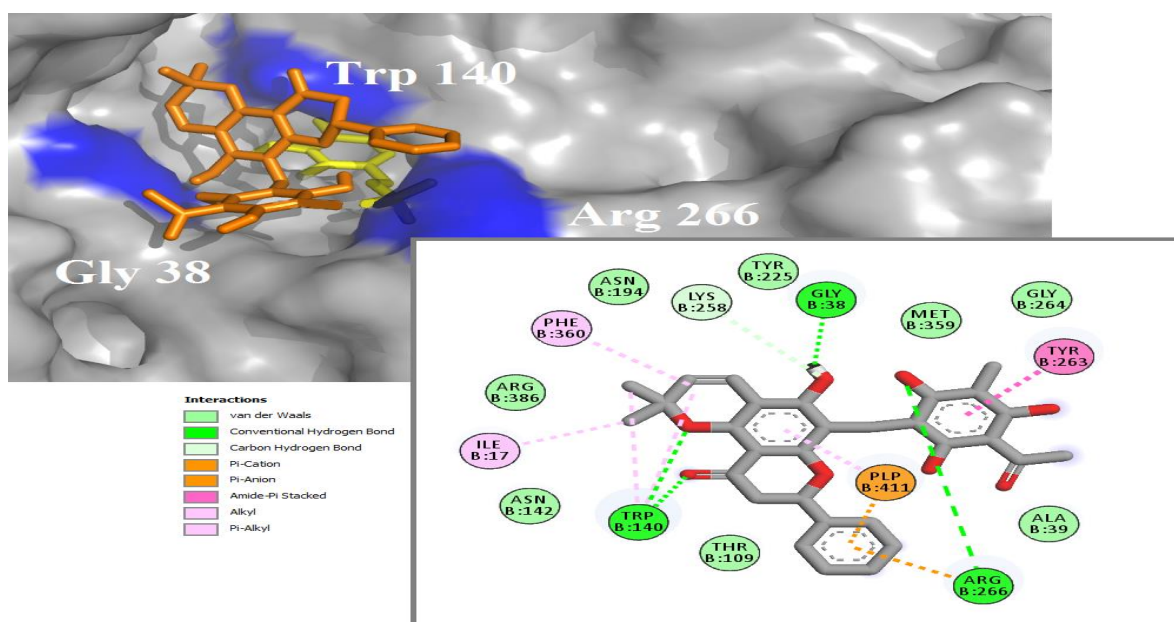


Figure 6. 2D and 3D views of the interaction between isorottlerin and the active site of aspartate aminotransferase (AST) and pyridoxal-5'-phosphate (PLP) are shown on a yellow stick.

To determine the drug-likeness properties of the retrieved potential inhibitors for both ALT and AST enzymes, the SwissADME webserver was used to ascertain the suitable ADME properties. The results were listed in Table 3 and Table 4, respectively [53].

Table 3. Calculated ADME properties of the top ten potential inhibitors of alanine aminotransferase (ALT).

Compound	MW (g/mol)	H bond acceptors	H bond donors	TPSA (Å ²)	MLOGP	Lipinski [54]	ESOL class [55]
Xanthurenic acid-β-glucoside	367.31	9	6	169.54	-2.08	Yes	Very soluble
Darutoside	484.62	8	6	139.84	0.65	Yes	Soluble
Dibenzoylgagaimol	606.70	9	5	153.75	2.65	Yes	Mod. Soluble
Kaempferol-3-robinobioside	593.51	15	8	252.03	-3.43	No	Soluble
Scoparin	461.40	11	6	193.11	-2.29	No	Soluble
7-methoxy-baicalein	591.54	14	6	220.80	-2.76	No	Soluble
Linarin	591.54	14	6	220.80	-2.76	No	Soluble
Glucan	504.44	16	11	268.68	-6.15	No	Highly soluble
Pseudomorphine	570.68	6	6	108.26	-5.13	No	Mod. soluble
Corilagin	634.45	18	11	310.66	-2.42	No	Soluble

Table 4. Calculated ADME properties of top ten potential inhibitors of aspartate aminotransferase (AST).

Compound	MW (g/mol)	H bond acceptors	H bond donors	TPSA (Å ²)	MLOGP	Lipinski [54]	ESOL class [55]
Xanthurenic acid-β-glucoside	367.31	9	6	169.54	-2.08	Yes	Very soluble
Isorottlerin	516.54	8	4	133.52	1.73	Yes	Poorly soluble
flavonol 3-o-glycosides	400.38	8	4	129.59	-0.6	Yes	Soluble
Scoparin	462.40	11	7	190.28	-2.29	No	Soluble
Glucononitol	208.25	5	5	101.15	-0.95	Yes	Highly soluble
Sucrose	342.30	11	8	189.53	-4.37	No	Highly soluble
Dibenzoylgagaimol	606.70	9	5	153.75	2.65	Yes	Mod. soluble
Lamiol	378.37	10	7	169.30	-2.71	Yes	Highly soluble
Kutkoside	512.46	13	6	197.13	-2.14	No	Very soluble
Lactulose	342.30	11	8	189.53	-4.37	No	Highly soluble

The ADME results indicated that all three compounds, xanthurenic acid- β -glucoside, darutoside, and isorottlerin obey almost all the rules in Lipinski's rule of five. However, xanthurenic acid- β -glucoside indicates superiority in terms of molecular weight of 367.31g/mol, six hydrogen bond donors, nine hydrogen bond acceptors, and LogP -2.08, which causes better solubility compared to darutoside, and isorottlerin. Besides, xanthurenic acid- β -glucoside showed the highest binding energy and proper interactions and effectiveness against both active sites of the ALT and AST.

Reported ALT inhibitors, including aminoxy acetate (AOA) [56], succinic acid [57], sitagliptin, and dapagliflozin reduce the levels of ALT. Furthermore, several chemicals have been identified to inhibit AST. The list includes vinyl glycine [58], alpha-methyl aspartate [59], gostatin [60]; besides hesperetin [61], hesperidin [62] is the common inhibitor for ALT and AST levels (Figure 7 A).

Figure 7 B and C, similar to the top three compounds obtained from docking results xanthurenic acid- β -glucoside, darutoside, and isorottlerin, the reported inhibitors of both ALT and AST enzymes are also placed on top of the cavity of the active site which carries the PLP moieties. This means that the inhibitory mechanism of discovered compounds and reported inhibitors are likely to be the same, and both groups may prevent the catalytic interaction of the enzyme by occupying the entrance space of the active site area. However, the docking binding energy of the reported inhibitors is significantly lower than the binding energy of the discovered inhibitors. This can be due to the larger size of the discovered compounds that contain different functional groups and can interact well with amino acids in the active site area. And therefore, they can probably perform their inhibitory effect more effectively than the reported inhibitors.

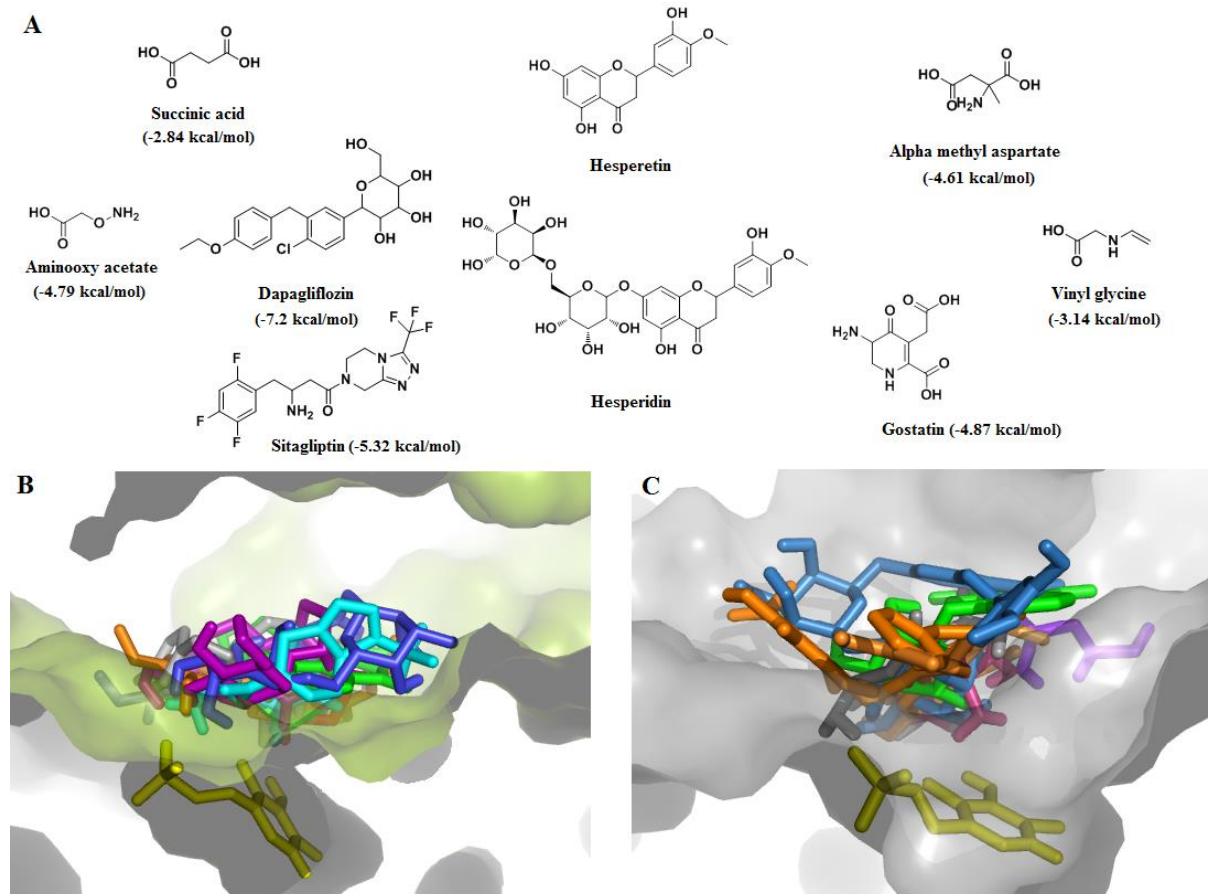


Figure 7. (A) Chemical structure of reported alanine aminotransferase (ALT) and aspartate aminotransferase (AST) inhibitors and related placement in the active site (B) and (C), respectively.

This is where the priority goes to three compounds, xanthurenic acid- β -glucoside, darutoside, and isorottlerin. Interacting with key residues in the active site better than other inhibitors and suitable ADME properties are advantages that make them a great clinical candidate for upcoming trials. Alternatively, the general structure can also be exploited for designing novel inhibitors.

4. Conclusions

In recent decades, chronic conditions related to the increase of ALT and AST in the human body have been emerging rapidly. Discovering novel ALT and AST inhibitors is mandatory for keeping human health away from immense harm in the future. We aimed to find potential inhibitors by using the large scales docking-based virtual screening method and ranking the compounds based on the docking binding energy arranged from the lowest to highest. The results revealed that the top first compound, xanthurenic acid- β -glucoside could fit well in the active site of both ALT and AST and may inhibit the catalysis process; besides, the proper ADME properties make it a great clinical option for upcoming trials and inhibiting the ALT and AST enzyme in chronic conditions afterward. Taking together all three selected compounds, xanthurenic acid- β -glucoside, darutoside, and isorottlerin can be promising for treating chronic conditions. Nevertheless, further clinical investigations are necessary to determine whether they can be effective in clinical situations.

Funding

This research was funded by the Tehran University of Medical Sciences and Health Services.

Acknowledgments

This publication was supported by Elite Researcher Grant Committee under award number [963465] from the National Institutes for Medical Research Development (NIMAD), Tehran, Iran.

Conflicts of Interest

The authors declare that they have no known competing financial interests or personal relationships that could have influenced the work reported in this paper.

References

1. Acharya, P.; Chouhan, K.; Weiskirchen, S.; Weiskirchen, R. Cellular Mechanisms of Liver Fibrosis. *Front Pharmacol* **2021**, *12*, 671640, <https://doi.org/10.3389/fphar.2021.671640>.
2. Polidoro, M.A.; Ferrari, E.; Marzorati, S.; Lleo, A.; Rasponi, M. Experimental liver models: From cell culture techniques to microfluidic organs-on-chip. *Liver Int* **2021**, *41*, 1744-1761, <https://doi.org/10.1111/liv.14942>.
3. De Anna, J.S.; Castro, J.M.; Darraz, L.A.; Elias, F.D.; Carcamo, J.G.; Luquet, C.M. Exposure to hydrocarbons and chlorpyrifos alters the expression of nuclear receptors and antioxidant, detoxifying, and immune response proteins in the liver of the rainbow trout, *Oncorhynchus mykiss*. *Ecotoxicol Environ Saf* **2021**, *208*, 111394, <https://doi.org/10.1016/j.ecoenv.2020.111394>.
4. Conway, M.E. Emerging Moonlighting Functions of the Branched-Chain Aminotransferase Proteins. *Antioxid Redox Signal* **2021**, *34*, 1048-1067, <https://doi.org/10.1089/ars.2020.8118>.
5. Jiang, Q.; Wang, L.; Si, X.; Tian, J.-L.; Zhang, Y.; Gui, H.-L.; Li, B.; Tan, D.-H. Current progress on the mechanisms of hyperhomocysteinemia-induced vascular injury and use of natural polyphenol compounds. *Eur J Pharmacol* **2021**, *905*, 174168, <https://doi.org/10.1016/j.ejphar.2021.174168>.
6. Khan, Y.M.; Khan, M.A. Optimization of dietary pyridoxine improved growth performance, hematological indices, antioxidant capacity, intestinal enzyme activity, non-specific immune response, and liver pyridoxine

- concentration of fingerling major carp *Catla catla* (Hamilton). *Aquaculture* **2021**, *541*, 736815, <https://doi.org/10.1016/j.aquaculture.2021.736815>.
7. Zheng, Q.; Wang, H.; Hou, W.; Zhang, Y. Use of Anti-angiogenic Drugs Potentially Associated With an Increase on Serum AST, LDH, CK, and CK-MB Activities in Patients With Cancer: A Retrospective Study. *Front Cardiovasc Med* **2021**, *8*, <https://doi.org/10.3389/fcvm.2021.755191>.
 8. Jung, J.I.; Lee, H.S.; Jeon, Y.E.; Kim, S.M.; Hong, S.H.; Moon, J.M.; Lim, C.Y.; Kim, Y.H.; Kim, E.J. Anti-inflammatory activity of palmitoylethanolamide ameliorates osteoarthritis induced by monosodium iodoacetate in Sprague-Dawley rats. *Inflammopharmacology* **2021**, *29*, 1475-1486, <https://doi.org/10.1007/s10787-021-00870-3>.
 9. Gao, G.; Sun, X.; Liu, X.; Jiang, Y.W.; Tang, R.; Guo, Y.; Wu, F.G.; Liang, G. Intracellular Nanoparticle Formation and Hydroxychloroquine Release for Autophagy-Inhibited Mild-Temperature Photothermal Therapy for Tumors. *Adv Funct Mater* **2021**, *31*, 2102832, <https://doi.org/10.1002/adfm.202102832>.
 10. Tian, S.; Jiang, X.; Tang, Y.; Han, T. Laminaria japonica fucoidan ameliorates cyclophosphamide-induced liver and kidney injury possibly by regulating Nrf2/HO-1 and TLR4/NF-kappaB signaling pathways. *J Sci Food Agric* **2022**, *102*, 2604-2612, <https://doi.org/10.1002/jsfa.11602>.
 11. Wang, Z.; Singh, R.; Marques, C.; Jha, R.; Zhang, B.; Kumar, S. Taper-in-taper fiber structure-based LSPR sensor for alanine aminotransferase detection. *Optics Express* **2021**, *29*, 43793-43810, <https://opg.optica.org/oe/fulltext.cfm?uri=oe-29-26-43793&id=466024>.
 12. Ntchapda, F.; Tchatchouang, F.C.; Miaffo, D.; Maidadi, B.; Vecchio, L.; Talla, R.E.; Bonabe, C.; Seke Etet, P.F.; Dimo, T. Hypolipidemic and anti-atherosclerogenic effects of aqueous extract of Ipomoea batatas leaves in diet-induced hypercholesterolemic rats. *J Integr Med* **2021**, *19*, 243-250, <https://doi.org/10.1016/j.joim.2021.02.002>.
 13. Albhaisi, S.; Qayyum, R. The association between serum liver enzymes and cancer mortality. *Clin Exp Med* **2022**, *22*, 75-81, <https://link.springer.com/article/10.1007/s10238-021-00733-9>.
 14. Jia, J.; Yang, Y.; Liu, F.; Zhang, M.; Xu, Q.; Guo, T.; Wang, L.; Peng, Z.; He, Y.; Wang, Y. The association between serum alanine aminotransferase and hypertension: a national based cross-sectional analysis among over 21 million Chinese adults. *BMC Cardiovascular Disorders* **2021**, *21*, 1-12, <https://bmccardiovascdisord.biomedcentral.com/articles/10.1186/s12872-021-01948-0>.
 15. He, Y.; Ding, F.; Yin, M.; Zhang, H.; Hou, L.; Cui, T.; Xu, J.; Yue, J.; Zheng, Q. High Serum AST/ALT Ratio and Low Serum INS* PA Product Are Risk Factors and Can Diagnose Sarcopenia in Middle-Aged and Older Adults. *Frontiers in Endocrinology* **2022**, *13*, <https://doi.org/10.3389/fendo.2022.843610>.
 16. De Matteis, C.; Cariello, M.; Graziano, G.; Battaglia, S.; Suppressa, P.; Piazzolla, G.; Sabbà, C.; Moschetta, A. AST to Platelet Ratio Index (APRI) is an easy-to-use predictor score for cardiovascular risk in metabolic subjects. *Sci Rep* **2021**, *11*, 1-14, <https://pubmed.ncbi.nlm.nih.gov/34290320/>.
 17. Rahman, S.; Islam, S.; Haque, T.; Kathak, R.R.; Ali, N. Association between serum liver enzymes and hypertension: a cross-sectional study in Bangladeshi adults. *BMC Cardiovasc Disord* **2020**, *20*, 1-7, <https://doi.org/10.1186/s12872-020-01411-6>.
 18. Cho, A.-R.; Lee, J.-H.; Kwon, Y.-J. Differences among Three Skeletal Muscle Mass Indices in Predicting Non-Alcoholic Fatty Liver Disease: Korean Nationwide Population-Based Study. *Life* **2021**, *11*, 751, <https://doi.org/10.3390%2Flife11080751>.
 19. He, M.M.; Fang, Z.; Hang, D.; Wang, F.; Polychronidis, G.; Wang, L.; Lo, C.H.; Wang, K.; Zhong, R.; Knudsen, M.D.; et al. Circulating liver function markers and colorectal cancer risk: A prospective cohort study in the UK Biobank. *Int J Cancer* **2021**, *148*, 1867-1878, <https://doi.org/10.1002/ijc.33351>.
 20. Changizi, Z.; Moslehi, A.; Rohani, A.H.; Eidi, A. Chlorogenic acid induces 4T1 breast cancer tumor's apoptosis via p53, Bax, Bcl-2, and caspase-3 signaling pathways in BALB/c mice. *Journal of Biochemical and Molecular Toxicology* **2021**, *35*, e22642, <https://doi.org/10.1002/jbt.22642>.
 21. Sun, Y.; Zhang, X.-X.; Huang, S.; Pan, H.; Gai, Y.-Z.; Zhou, Y.-Q.; Zhu, L.; Nie, H.-Z.; Li, D.-X. Diet-Induced Obesity Promotes Liver Metastasis of Pancreatic Ductal Adenocarcinoma via CX3CL1/CX3CR1 Axis. *Journal of immunology research* **2022**, *2022*, <https://doi.org/10.1155/2022/5665964>.
 22. Tarannum, M.; Hossain, M.A.; Holmes, B.; Yan, S.; Mukherjee, P.; Vivero-Escoto, J.L. Advanced Nanoengineering Approach for Target-Specific, Spatiotemporal, and Ratiometric Delivery of Gemcitabine-Cisplatin Combination for Improved Therapeutic Outcome in Pancreatic Cancer. *Small* **2022**, *18*, e2104449, <https://doi.org/10.1002/sml.202104449>.
 23. Ndrepepa, G. Aspartate aminotransferase and cardiovascular disease—a narrative review. *J. Lab. Precis. Med* **2021**, *6*, <https://jlp.amegroups.com/article/view/5898/html>.
 24. Madhavan, A.; Kok, B.P.; Rius, B.; Grandjean, J.M.D.; Alabi, A.; Albert, V.; Sukiasyan, A.; Powers, E.T.; Galmozzi, A.; Saez, E.; et al. Pharmacologic IRE1/XBP1s activation promotes systemic adaptive remodeling in obesity. *Nat Commun* **2022**, *13*, 608, <https://doi.org/10.1038/s41467-022-28271-2>.
 25. Qu, X.; Guan, P.; Xu, L.; Liu, B.; Li, M.; Xu, Z.; Huang, X.; Han, L. Riligustilide alleviates hepatic insulin resistance and gluconeogenesis in T2DM mice through multitarget actions. *Phytother Res* **2022**, *36*, 462-474, <https://doi.org/10.1002/ptr.7346>.

26. Li, X.; Jayachandran, M.; Xu, B. Antidiabetic effect of konjac glucomannan via insulin signaling pathway regulation in high-fat diet and streptozotocin-induced diabetic rats. *Food Research International* **2021**, *149*, 110664, <https://doi.org/10.1016/j.foodres.2021.110664>.
27. Moreno, J.C.; Rojas, B.E.; Vicente, R.; Gorka, M.; Matz, T.; Chodasiewicz, M.; Peralta-Ariza, J.S.; Zhang, Y.; Alseekh, S.; Childs, D. Moreno JC, Rojas BE, Vicente R, Gorka M, Matz T, Chodasiewicz M, Peralta-Ariza JS, Zhang Y, Alseekh S, Childs D, Luzarowski M. Tyr-Asp inhibition of glyceraldehyde 3-phosphate dehydrogenase affects plant redox metabolism. *The EMBO journal*. **2021** Aug 2;40 (e106800). <https://doi.org/10.15252/embj.2020106800>. *The EMBO journal* **2021**, *40*, e106800.
28. Obeid, M.; Kazi, M. Plasmapheresis as a treatment of thyrotoxicosis in pregnancy: Case report. *J Clin Transl Endocrinol* **2022**, *24*, 100110.
29. Floresta, G.; Crocetti, L.; Giovannoni, M.P.; Biagini, P.; Cilibrizzi, A. Repurposing strategies on pyridazinone-based series by pharmacophore-and structure-driven screening. *Journal of enzyme inhibition and medicinal chemistry* **2020**, *35*, 1137-1144, <https://doi.org/10.1080/14756366.2020.1760261>.
30. Choi, B.H.; Coloff, J.L. The Diverse Functions of Non-Essential Amino Acids in Cancer. *Cancers (Basel)* **2019**, *11*, 675, <https://doi.org/10.3390/cancers11050675>.
31. Lin, L.; Fu, P.; Chen, N.; Gao, N.; Cao, Q.; Yue, K.; Xu, T.; Zhang, C.; Zhang, C.; Liu, F.; et al. Total flavonoids of *Rhizoma Drynariae* protect hepatocytes against aflatoxin B1-induced oxidative stress and apoptosis in broiler chickens. *Ecotoxicol Environ Saf* **2022**, *230*, 113148, <https://doi.org/10.1016/j.ecoenv.2021.113148>.
32. Zareei, S.; Boojar, M.M.A.; Amanlou, M. Inhibition of liver alanine aminotransferase and aspartate aminotransferase by hesperidin and its aglycone hesperetin: An in vitro and in silico study. *Life Sci* **2017**, *178*, 49-55, <https://doi.org/10.1016/j.lfs.2017.04.001>.
33. Novick, P.A.; Ortiz, O.F.; Poelman, J.; Abdulhay, A.Y.; Pande, V.S. SWEETLEAD: an in silico database of approved drugs, regulated chemicals, and herbal isolates for computer-aided drug discovery. *PLoS One* **2013**, *8*, e79568, <https://doi.org/10.1371/journal.pone.0079568>.
34. Morris, G.M.; Huey, R.; Lindstrom, W.; Sanner, M.F.; Belew, R.K.; Goodsell, D.S.; Olson, A.J. AutoDock4 and AutoDockTools4: Automated docking with selective receptor flexibility. *J Comput Chem* **2009**, *30*, 2785-2791, <https://doi.org/10.1002/jcc.21256>.
35. O'Boyle, N.M.; Banck, M.; James, C.A.; Morley, C.; Vandermeersch, T.; Hutchison, G.R. Open Babel: An open chemical toolbox. *J Cheminform* **2011**, *3*, 33, <https://doi.org/10.1186/1758-2946-3-33>.
36. Hosseini, F.S.; Amanlou, M. Anti-HCV and anti-malaria agent, potential candidates to repurpose for coronavirus infection: Virtual screening, molecular docking, and molecular dynamics simulation study. *Life Sci* **2020**, *258*, 118205, <https://doi.org/10.1016/j.lfs.2020.118205>.
37. Hosseini, F.S.; Amanlou, A.; Amanlou, M. Tankyrase Inhibitor for Cardiac Tissue Regeneration: an In-silico Approach. *Iran J Pharm Res* **2021**, *20*, 315-328, <https://doi.org/10.22037/ijpr.2021.115367.15339>.
38. Kazemzadeh, H.; Hamidian, E.; Hosseini, F.S.; Abdi, M.; Niasari Naslaji, F.; Talebi, M.; Asadi, M.; Biglar, M.; Zarei, I.; Amanlou, M. Isoindolin-1-ones Fused to Barbiturates: From Design and Molecular Docking to Synthesis and Urease Inhibitory Evaluation. *ACS Omega* **2022**, *7*, 19401-19411, <https://doi.org/10.1021/acsomega.2c01028>.
39. Mohseni, M.; Bahrami, H.; Farajmand, B.; Hosseini, F.S.; Amanlou, M.; Salehabadi, H. Indole alkaloids as potential candidates against COVID-19: an in silico study. *Journal of molecular modeling* **2022**, *28*, 1-13, <https://doi.org/10.1007/s00894-022-05137-4>.
40. Studio, D. Dassault systemes BIOVIA, Discovery studio modelling environment, Release 4.5. *Accelrys Softw Inc* **2015**, 98-104.
41. Schrödinger, L. The PyMOL molecular graphics system, version 1.7. 6.6. *Schrödinger LLC* **2015**.
42. Bujacz, A.; Rum, J.; Rutkiewicz, M.; Pietrzyk-Brzezinska, A.J.; Bujacz, G. Structural Evidence of Active Site Adaptability towards Different Sized Substrates of Aromatic Amino Acid Aminotransferase from *Psychrobacter* Sp. B6. *Materials (Basel)* **2021**, *14*, 3351, <https://doi.org/10.3390/ma14123351>.
43. Jeong, S.Y.; Jin, H.; Chang, J.H. Crystal structure of L-aspartate aminotransferase from *Schizosaccharomyces pombe*. *PLoS One* **2019**, *14*, e0221975, <https://doi.org/10.1371/journal.pone.0221975>.
44. McPhalen, C.A.; Vincent, M.G.; Jansonius, J.N. X-ray structure refinement and comparison of three forms of mitochondrial aspartate aminotransferase. *J Mol Biol* **1992**, *225*, 495-517, [https://doi.org/10.1016/0022-2836\(92\)90935-d](https://doi.org/10.1016/0022-2836(92)90935-d).
45. Ford, G.C.; Eichele, G.; Jansonius, J.N. Three-dimensional structure of a pyridoxal-phosphate-dependent enzyme, mitochondrial aspartate aminotransferase. *Proc Natl Acad Sci U S A* **1980**, *77*, 2559-2563, <https://doi.org/10.1073/pnas.77.5.2559>.
46. Nero, T.L.; Wong, M.G.; Oliver, S.W.; Iskander, M.N.; Andrews, P.R. Aspartate aminotransferase: investigation of the active sites. *J Mol Graph* **1990**, *8*, 111-115, 192-113, [https://doi.org/10.1016/0263-7855\(90\)80091-s](https://doi.org/10.1016/0263-7855(90)80091-s).
47. Azadmanesh, J.; Lutz, W.E.; Coates, L.; Weiss, K.L.; Borgstahl, G.E.O. Cryotrapping peroxide in the active site of human mitochondrial manganese superoxide dismutase crystals for neutron diffraction. *Acta Crystallogr F Struct Biol Commun* **2022**, *78*, 8-16, <https://doi.org/10.1107/S2053230X21012413>.

48. Bonnard, M.; Boury, B.; Parrot, I. Xanthurenic Acid in the Shell Purple Patterns of *Crassostrea gigas*: First Evidence of an Ommochrome Metabolite in a Mollusk Shell. *Molecules* **2021**, *26*, 7263, <https://doi.org/10.3390/molecules26237263>.
49. Xu, Y.; Feng, W.; Zhou, Q.; Liang, A.; Li, J.; Dai, A.; Zhao, F.; Yan, J.; Chen, C.-W.; Li, H. A distinctive ligand recognition mechanism by the human vasoactive intestinal polypeptide receptor 2. *Nature communications* **2022**, *13*, 1-10, <https://www.nature.com/articles/s41467-022-30041-z>.
50. Li, Y.S.; Zhang, J.; Tian, G.H.; Shang, H.C.; Tang, H.B. Kirenol, darutoside and hesperidin contribute to the anti-inflammatory and analgesic activities of *Siegesbeckia pubescens* makino by inhibiting COX-2 expression and inflammatory cell infiltration. *J Ethnopharmacol* **2021**, *268*, 113547, <https://doi.org/10.1016/j.jep.2020.113547>.
51. Zaidi, S.F.; Yoshida, I.; Butt, F.; Yusuf, M.A.; Usmanhani, K.; Kadowaki, M.; Sugiyama, T. Potent bactericidal constituents from *Mallotus philippinensis* against clarithromycin and metronidazole resistant strains of Japanese and Pakistani *Helicobacter pylori*. *Biol Pharm Bull* **2009**, *32*, 631-636, <https://doi.org/10.1248/bpb.32.631>.
52. Hong, Q.; Minter, D.E.; Franzblau, S.G.; Arfan, M.; Amin, H.; Reinecke, M.G. Anti-tuberculosis compounds from *Mallotus philippinensis*. *Nat Prod Commun* **2010**, *5*, 211-217, <https://doi.org/10.1177/1934578X1000500208>.
53. Daina, A.; Michielin, O.; Zoete, V. SwissADME: a free web tool to evaluate pharmacokinetics, drug-likeness and medicinal chemistry friendliness of small molecules. *Scientific reports* **2017**, *7*, 1-13, <https://www.nature.com/articles/srep42717>.
54. Moriguchi, I.; HIRONO, S.; LIU, Q.; NAKAGOME, I.; MATSUSHITA, Y. Simple method of calculating octanol/water partition coefficient. *Chem Pharm Bull* **1992**, *40*, 127-130, <https://doi.org/10.1016/j.jfoodeng.2003.10.015>.
55. Delaney, J.S. ESOL: estimating aqueous solubility directly from molecular structure. *J Chem Inf Comput Sci* **2004**, *44*, 1000-1005, <https://doi.org/10.1021/ci034243x>.
56. Rognstad, R.; Clark, D.G. Effects of aminooxyacetate on the metabolism of isolated liver cells. *Arch Biochem Biophys* **1974**, *161*, 638-646, [https://doi.org/10.1016/0003-9861\(74\)90348-8](https://doi.org/10.1016/0003-9861(74)90348-8).
57. Vyshtakalyuk, A.B.; Parfenov, A.A.; Gumarova, L.F.; Khasanshina, L.R.; Belyaev, G.P.; Nazarov, N.G.; Kondrashina, D.A.; Galyametdinova, I.V.; Semenov, V.E.; Zobov, V.V. Conjugate of pyrimidine derivative, the drug xymedon with succinic acid protects liver cells. *J Biochem Mol Toxicol* **2021**, *35*, e22660, <https://doi.org/10.1002/jbt.22660>.
58. Gehring, H.; Rando, R.R.; Christen, P. Active-site labeling of aspartate aminotransferases by the beta,gamma-unsaturated amino acid vinylglycine. *Biochemistry* **1977**, *16*, 4832-4836, <https://doi.org/10.1021/bi00641a012>.
59. Hammes, G.G.; Haslam, J.L. A kinetic investigation of the interaction of alpha-methylaspartic acid with aspartate aminotransferase. *Biochemistry* **1968**, *7*, 1519-1525, <https://doi.org/10.1021/bi00844a039>.
60. Kitagishi, K.; Hiromi, K.; Tanase, S.; Nagashima, F.; Morino, Y.; Nishino, T.; Murao, S. Kinetic studies on the binding of gostatin, a suicide substrate for aspartate aminotransferase, with the isoenzymes from porcine heart mitochondria and cytosol. *J Biochem* **1988**, *103*, 585-588, <https://doi.org/10.1093/oxfordjournals.jbchem.a122311>.
61. Li, J.; Wang, T.; Liu, P.; Yang, F.; Wang, X.; Zheng, W.; Sun, W. Hesperetin ameliorates hepatic oxidative stress and inflammation via the PI3K/AKT-Nrf2-ARE pathway in oleic acid-induced HepG2 cells and a rat model of high-fat diet-induced NAFLD. *Food Funct* **2021**, *12*, 3898-3918, <https://doi.org/10.1039/d0fo02736g>.
62. Famurewa, A.C.; Renu, K.; Eladl, M.A.; Chakraborty, R.; Myakala, H.; El-Sherbiny, M.; Elsherbini, D.M.A.; Vellingiri, B.; Madhyastha, H.; Wanjari, U.R. Hesperidin and hesperetin against heavy metal toxicity: Insight on the molecular mechanism of mitigation. *Biomedicine & Pharmacotherapy* **2022**, *149*, 112914, <https://doi.org/10.1016/j.biopha.2022.112914>.